MILITARY TECHNICAL COLLEGE

CAIRO - EGYPT

# AN EXPERIMENTAL INVESTIGATION ON A MANOEUVRING STRAKE-WING-BODY CONFIGURATION

A.M. AL-BAHI*, M.S. ALY*, M.M. ABDELRAHMAN* AND M.A. GHAZI*

## ABSTRACT

The aerodynamic characteristics of a tailless Strake-Wing-Body configuration are studied experimentally in a low speed wind tunnel. The model is mounted on a six component sting wind tunnel balance system to measure longitudinal and lateral forces and moments. Both sideslip and bank angles are varied independently for angles of attack up to 20 degrees. The effect of freestream Reynolds number is also considered. The study reveals that the strake vortex tends to delay wing vortex breakdown caused by small variations in sideslip and/or banking angles. Meanwhile, large lateral manoeuvres at low speeds must be executed at high angles of attack in order to compensate the loss in the lift coefficient. The study also demonstrates that the bank angle slightly degrades the stability margin and displaces the equilibrium point towards negative lift coefficients. The sideslip angle adds a constant negative side force, a positive yawing moment at low angles of attack and a negative yawing moment at high angles of attack. Also a negative stabilizing rolling moment is added by the bank and sideslip angles at moderate and high angles of attack.

## INTRODUCTION

Many modern aircraft and missiles designed for supersonic speeds employ highly swept back and low aspect ratio wings with sharp edges. However, such wings are inefficient in subsonic and high lift regimes, such as climb to cruise, manoeuvre and approach to landing, and have serious performance, stability and control deficiencies [1]. When the applications of such configurations were introduced, Earnshaw and Lawford [2] carried out some low-speed wind tunnel experiments on a series of delta wings. Wentz and McMahon [3] investigated the flow field about delta and double delta wings at low speeds. Rolls and Koenig [4] studied the aerodynamic properties of the ogee wing. These studies confirm that, at subsonic speeds, both the ogee wing and double-delta planforms exhibit a stable vortex phenomenon on the wing thereby reducing the aircraft landing speed. The name "Strake-wing combination" has been attributed, later on, to these planforms composed of a wing and a small highly swept area ahead of its leading edge.

*Aeronautical Eng. Dept., King AbdulAziz Univ.,
P. O. Box 9027, Jeddah 21413, Saudi Arabia

Strake-wing combinations have been investigated quite extensively in the last decade [5-8]. It has been established that strakes produce favorable effects at high angles of attack in subsonic and transonic flight regimes. They positively affect leeside flow separation and vortex breakdown of moderate sweep wings. These strake effects [9-10] result from the strong leading-edge vortices generated by the strake which induce an outboard flow on the main wing and thereby increase the effective sweep of the leading edge. The higher effective sweep stabilizes the leading edge separation on the main wing and, consequently, increases the onset angle of attack for vortex breakdown. As noticed by Stallings [11], the major advantage of the strake-wing combination is that favorable interference is created at high lift conditions without degrading the wing performance at lower angles of attack.

Low speed wind-tunnel investigations [12-13] on double-delta wings indicate that at low angles of attack two primary vortices are shed leeward on each side of the wing, originating from the leading edges of both strake and wing, and remain distinguishable over the entire wing. At medium angles of attack, they wrap around each other and merge into one stable vortex over the rear part of the wing. At high angles of attack, they merge right after the kink and no longer separate. At very high angles of attack, the large-scale vortex breakdown occurs over the wing and the induced vortical lift diminishes.

Hoeijmakers et al. [14] presented a theoretical and experimental investigation of the flow about a slender wing and two double-delta wings. Their investigation indicated that the flow pattern above sharp edged double-delta wings consists of a single-branched strake vortex and a double-branched wing vortex. Numerical results were obtained for the flow about 76-deg. swept delta wing using a free vortex sheet method for the fully three-dimensional problem. In fact the low speed vortical interaction phenomenon has motivated development of some fast and reliable computational methods for three dimensional incompressible flow. Among those, an implicit finite difference scheme was used by Hsu et al. [15] to compute the three dimensional incompressible laminar vortical flow around a sharp-edged double-delta wing with an aspect ratio of 2.06. By adding a time derivative of the pressure to the continuity equation, the unsteady incompressible Navier-Stockes equations can be integrated like a conventional parabolic time-dependent system of equations. Numerical results indicate that the second-order-accurate scheme has successfully simulated the vortical interaction between the strake and wing vortices.

Although several references are available in the literature concerning different strake-wing design aspects [7,16-17], existing performance studies are generally limited to the case of symmetric, longitudinal flight conditions. The effect of non-symmetric incident flow, such as sideslip and banking, on the interaction between the strake vortex and the wing leeside flow seems to represent a gap in the open literature of experimental studies. Meanwhile the numerical simulation of such manoeuvres remains beyond the capability of existing numerical techniques.

In the present work, the aerodynamic forces and moments on a manoeuvring strake-wing-body configuration are studied in a low speed wind tunnel. Both sideslip and bank angles of the model are varied independently. The forces and moments are measured for angles of attack up to 20 degrees. The effect of freestream Reynolds number is also considered.

## Experimental Setup and Measurements

Experiments are performed in a low speed, 700X500 mm, open circuit wind tunnel. The model consists of a sharp-edged flat plate strake-wing combination with an aspect ratio of 1.84, root chord of 264 mm, span of 230 mm, uniform thickness of 3 mm and symmetrical, wedge-shaped (apex angle of 30 deg.) leading and trailing edges (see Fig. 1). The fuselage of the actual configuration was approximated by a cylindrical body with a pointed nose. The cylindrical part features 258 mm length and 32mm diameter while the conical part smoothly matches the cylinder and has 99 mm length. The strake approaches that of the F16 fighter aircraft ahead of a trapezoidal wing of 40 deg. leading edge sweepback angle.

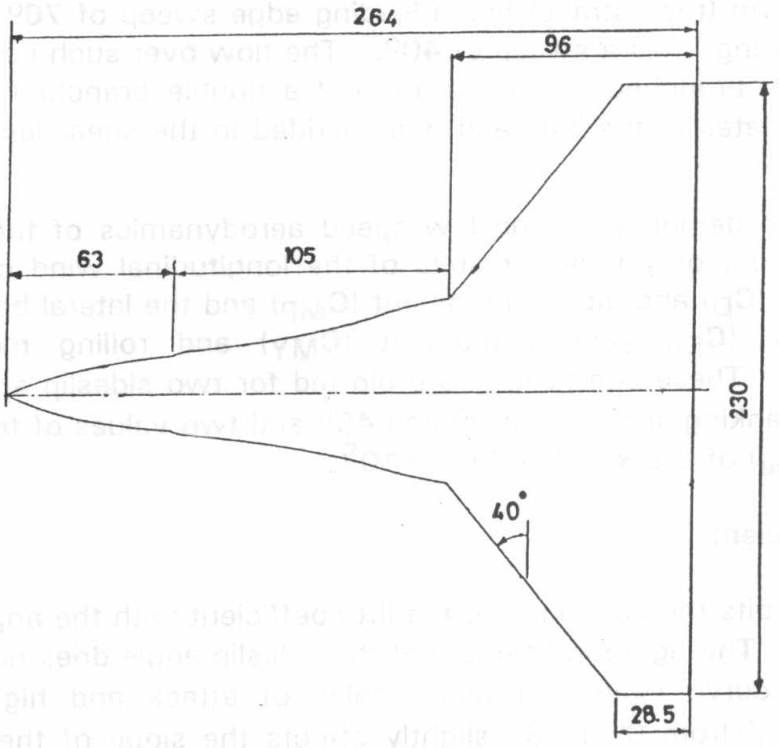


**Fig. 1 Planform of the strake-wing combination.**

The model is mounted on a six component sting wind tunnel balance system. An HP data acquisition system is integrated with the electronic part of wind tunnel balance for gathering and presentation of data. Sensitive pressure differential electronic micromanometers are used for measuring free-stream velocity.

In order to simulate different manoeuvres, the banking angle, $\phi$, was varied between 0 and 90 degrees at a step of 10 degrees while the sideslip angle, $\beta$, was varied between 0 and 12 degrees at a step of 2 degrees. Lift, drag and side forces together with yawing, pitching and rolling moments were measured for angles of attack ranging from 0 to 20 degrees. Measurements were taken for two values of the free stream velocity of 20 and 30 m/s, corresponding to Reynolds numbers based on wing root chord of $3.6 \times 10^5$ and $5.5 \times 10^5$ respectively.

## RESULTS AND DISCUSSION

The studied strake-wing configuration can be idealized by a double delta wing approaching model III of Hoeijmakers et al. [14], in which the forward half of the planform (the strake) has a leading edge sweep of $76^o$ while the rearward half (the wing ) has a sweep of $40^o$. The flow over such configuration consists of a single-branched strake vortex and a double branched wing vortex. The later originates at the kink and is embedded in the shear layer from the leading edge.

In order to demonstrate the low speed aerodynamics of the strake-wing-body configuration, only typical results of the longitudinal wind coefficients, i.e. lift ($C_L$), drag ($C_D$) and pitching moment ($C_{MP}$) and the lateral body coefficients i.e. side force ($C_S$), yawing moment ($C_{MY}$) and rolling moment ($C_{MR}$) are presented. These coefficients are plotted for two sideslip angles ($\beta$) of $0^o$ and $8^o$, two banking angle ($\phi$) of $0^o$ and $45^o$ and two values of freestream Reynolds number ($R_e$) of $3.6 \times 10^5$ and $5.5 \times 10^5$.

### Lift Coefficient

Fig. 2 exhibits the variations of the lift coefficient with the angle of attack of the model ($\alpha$). The figure indicates that the sideslip angle does not practically affect the $C_L$-$\alpha$ curve except at high angles of attack and high banking angles. Increasing $\beta$ from $0^o$ to $8^o$ slightly affects the slope of the linear part of the curve ($dC_L/d\alpha$), while increasing $\phi$ from $0^o$ to $45^o$ considerably decreases this slope. In fact the lifting force is largely affected by the vortex breakdown (VB) and its position on the upper surface of the planform [18]. In the flow conditions where VB is not present over the wing (moderate $\alpha$ and small $\beta$ and $\phi$), the suction induced by the leading edge vortices increases steadily with the angle of attack. Down-stream of VB point there is a reduction in the rate of

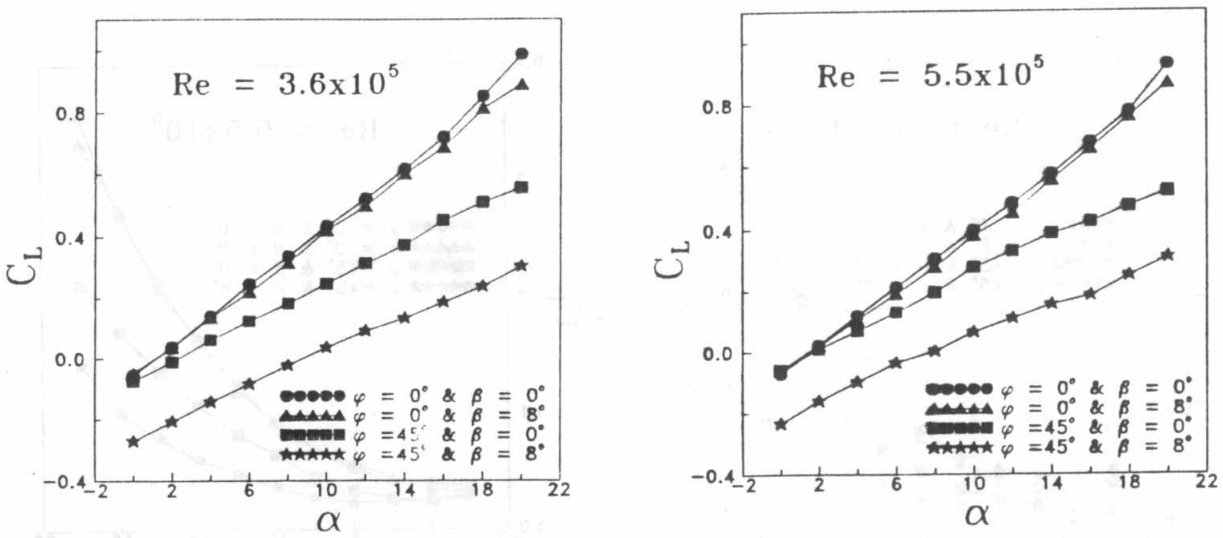


**Fig. 2 Variations of the lift coefficient during lateral manoeuvres.**

change of the peak suction with the incidence angle. Meanwhile the VB point moves further upstream as $\alpha$ increases. It seems that the strake vortex tends to delay wing vortex breakdown caused by both small variations in $\beta$ and $\phi$.

It is also noticed from Fig. 2 that, at constant angle of attack, increasing the sideslip angle decreases the lift coefficient specially at high banking angles. By consequence, the zero lift angle of attack ($\alpha_{L=0}$) and the maximum lift coefficient ($C_{Lmax}$) increase with the increase of $\beta$ and $\phi$.

As expected the effect of Reynolds number ($R_e$) is very small since the two values investigated are of the same order of magnitude. Nevertheless, it can be easily concluded from the figure that the above mentioned effects of $\beta$ and $\phi$ on $C_L$-$\alpha$ curve are more pronounced at lower Reynolds numbers. By consequence, at low Reynolds numbers and high sideslip or banking angles it is imperative to increase the angle of attack in order to compensate the loss in the lift coefficient. In other words, lateral manoeuvres at low speeds must be executed at high angles of attack.

**Drag coefficient**

$C_D$-$\alpha$ curves of Fig. 3 demonstrate that, similar to the case of the lift coefficient, the sideslip angle, $\beta$ does not affect $C_D$-$\alpha$ curves except at high banking angles. At these high values of $\phi$ increasing $\beta$ decreases, only, the high angles of attack drag coefficient. The drag values at low angles of attack either remain constants or increases with the increase of $\beta$. As $\beta$ or $\phi$ increases the minimum drag angle of attack, $^{\alpha}C_{Dmin}$, increases while the value of the minimum drag $C_{Dmin}$ decreases.

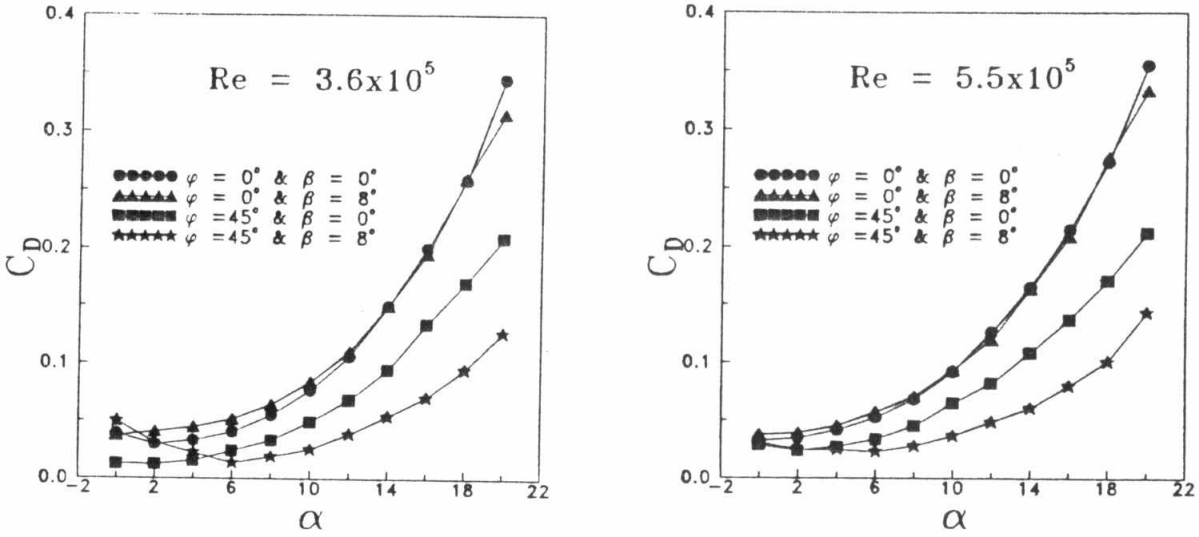


Fig. 3 Drag coefficient versus angle of attack variations.

The above conclusions are reflected on the drag polars $C_L$-$C_D$ represented in Fig. 4. The figure indicates that the maximum lift to drag ratio, $(C_L/C_D)_{max}$, decreases as $\beta$ or $\phi$ increases. In addition it appears that the drag at zero lift and the value of the lift at the minimum drag point are less affected by lateral manoeuvres, specially at high Reynolds numbers.

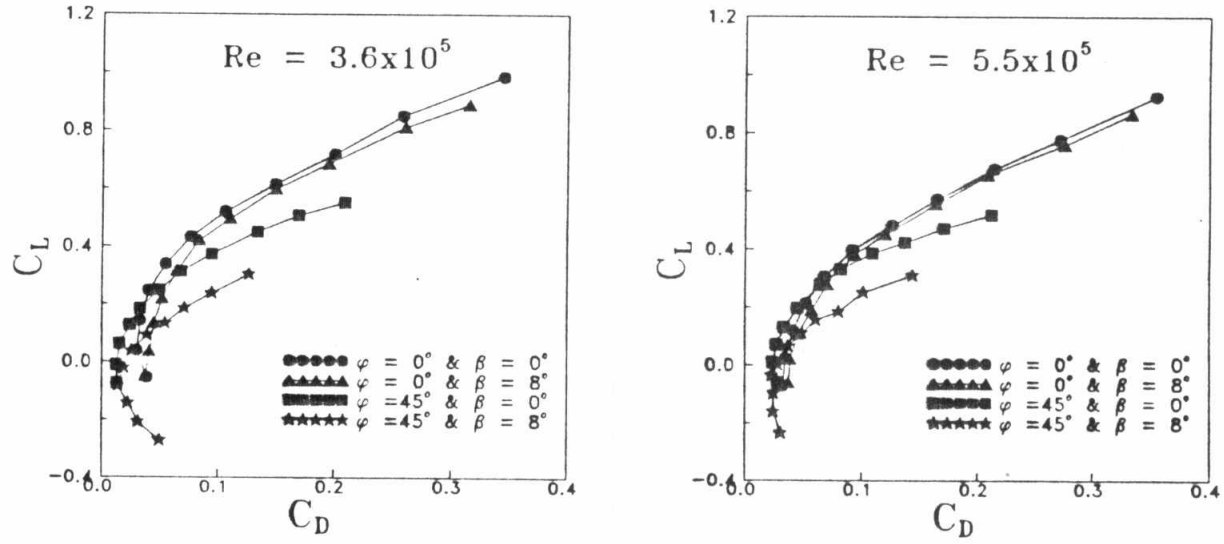


Fig. 4 Drag polar for different bank and sideslip angles.

**Pitching moment coefficient**

In Fig. 5 variations of the pitching moment coefficient are plotted against the lift coefficient during lateral manoeuvres. It is observed from the figure that the major effect on the equilibrium point and the stability margin, of this tailless configuration, arises from the bank angle contribution. This contribution slightly degrades the stability margin and displaces the equilibrium point towards negative lift coefficients. In fact at a constant angle of attack, the effect of $\phi$ is to decrease the lift coefficient and add a smaller negative (nose down) pitching moment such that the $C_{MP}$-$C_L$ curve is shifted towards lower $C_L$ values. On the other hand since the decrease in the lifting force due to $\phi$ is more pronounced at high angles of attack (see Fig. 2), the slope of $C_{MP}$-$C_L$ becomes more positive with $\phi$. The figure also demonstrates that the effect of the sideslip angle $\beta$ is only noticed at low Reynolds numbers where the increase of the sideslip angle tends to degrade the stability margin but slightly affects the equilibrium point.

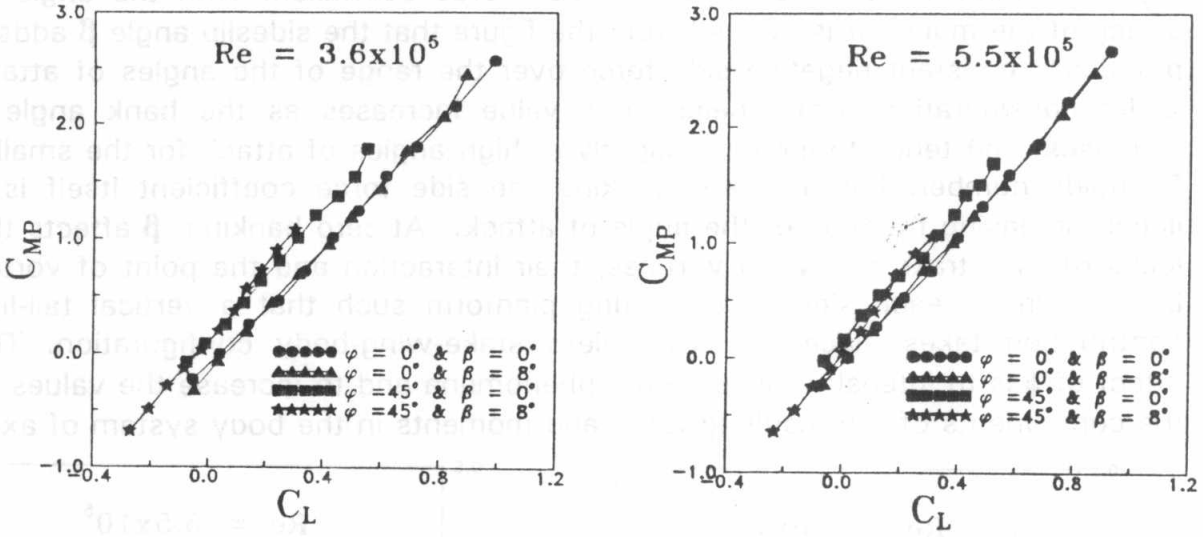


**Fig. 5 Longitudinal stability of the strake-wing-body configuration.**

On the other hand Fig. 6 shows that, at constant angles of attack and high bank angles, the pitching moment decreases i.e., a considerable amount of nose down pitching moment is added when $\beta$ increases. Meanwhile at zero banking and constant $\alpha$, $\beta$ has no effect on the pitching moment coefficient of the model.

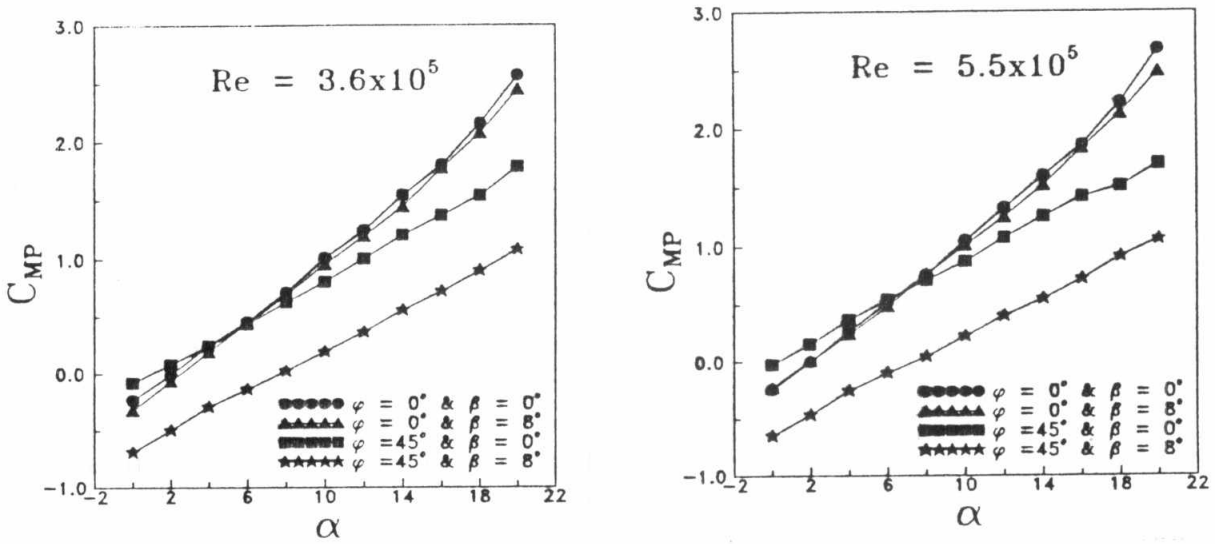


Fig. 6 Variations of the pitching moment coefficient.

Side force coefficient

Fig. 7 elucidates the variation of the side force coefficient with the angle of attack of the model. It is noticed from the figure that the sideslip angle $\beta$ adds a practically constant negative side force over the range of the angles of attack under consideration. Nevertheless this value increases as the bank angle $\phi$ increases and tends to increase slightly at high angles of attack for the smaller Reynolds number. For non-zero banking the side force coefficient itself is a linear increasing function of the angle of attack. At zero banking, $\beta$ affects the locus of the strake and wing vortices, their interaction and the point of vortex breakdown on each side of the lifting planform such that a vertical tail-like contribution takes place on this tailless stake-wing-body configuration. The effect of $\phi$ is to intensify these vortex phenomena and to increase the values of the components of the resulting force and moments in the body system of axes.

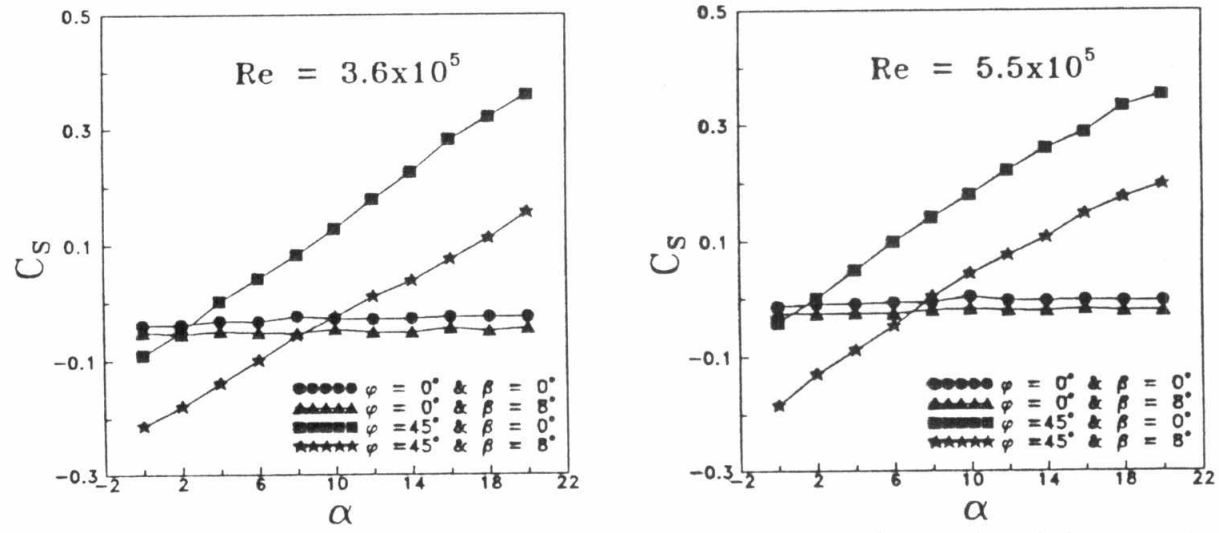


Fig. 7 Side force coefficient induced by lateral manoeuvres.

## Rolling Moment Coefficient

Fig. 8 demonstrates the variations of the rolling moment coefficient. The main observation in this figure is the negative stabilizing roll added by the banking angle, $\phi$, and the sideslip angle, $\beta$, at moderate and high angles of attack, $\alpha$. In this configuration the lift increases with $\alpha$ on the leading wing half (port wing) and becomes higher than the lift on the starboard wing impeded in the wake of the fuselage, such that a negative rolling moment is produced. The amount of this added rolling moment per sideslip angle is higher for higher bank angles, While at low angles of attack the contribution of $\beta$ and $\phi$ is small. The variations of the roll stability derivatives with the angle of attack at **Re** = 3.6 $10^5$ are shown in table 1. It is also concluded from the figure that the effect of lateral manoeuvres on the rolling moment is somewhat intensified at low Reynolds numbers.

**Table 1. Rolling and yawing stability derivatives (Re = $3.6 \times 10^5$)**

| | $\alpha = 10^o$ | $\alpha = 20^o$ |
|---|---|---|
| $(dC_{MR} / d\beta)_{\phi=0}$ | -0.029/rad | -0.057/rad |
| $(dC_{MR} / d\phi)_{\beta=0}$ | -0.014/rad | -0.033/rad |
| $(dC_{MY} / d\beta)_{\phi=0}$ | -0.039/rad | -0.152/rad |
| $(dC_{MY} / d\phi)_{\beta=0}$ | +0.005/rad | -0.051/rad |

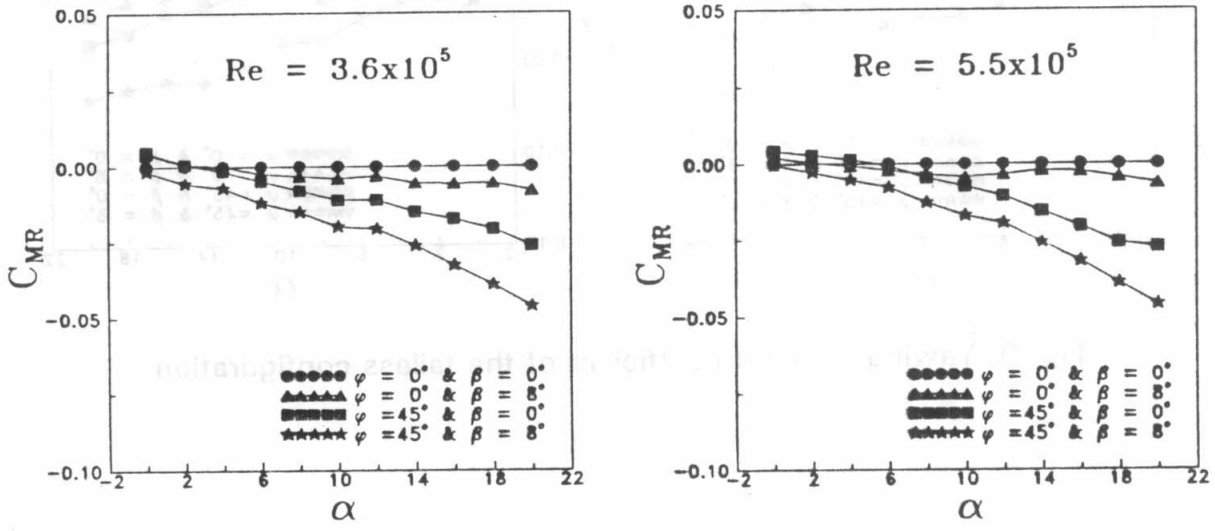


**Fig. 8 Rolling moment coefficient of the tailless configuration.**

### Yawing Moment Coefficient

Fig. 9 represents the yawing moment coefficient of the manoeuvring configuration. The figure indicates that the contribution of $\beta$ is to add a negative (anticlockwise) yawing moment. Similar to the case of rolling moment, the drag-due-to lift increases on the leading wing half (port wing) and becomes higher than the drag-due-to-lift on the starboard wing impeded in the wake of the fuselage, such that a negative yawing moment is produced. The amount of this stabilizing yawing moment per sideslip angle is higher for higher bank angles similar to the cases of side force and rolling moment. The contribution of $\phi$ is to add a positive yawing moment at low angles of attack and a negative yawing moment at high angles of attack. The angle of attack for which the change in $\phi$ has no yawing moment contribution depends, mainly, on the sideslip angle, $\beta$, and, to a very small extend, on the Reynolds number, **Re**. The variations of the yawing stability derivatives with the angle of attack at **Re** = $3.6 \times 10^5$ are shown in table 1.

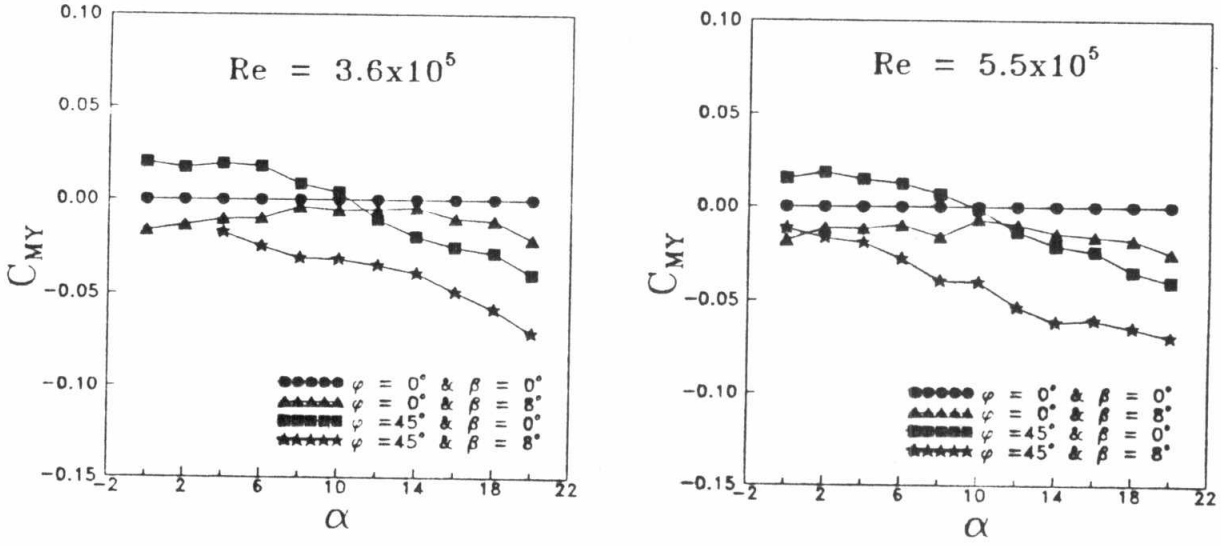


**Fig. 9 Yawing moment coefficient of the tailess configuration.**

## CONCLUSIONS

The aerodynamic characteristics of a tailless Strake-Wing-Body configuration are studied experimentally in a low speed wind tunnel. From the present investigation an insight has been gained into the performance of this supersonic planform at low speeds, during longitudinal and lateral manoeuvres. From the measurements of the resulting forces and moments, the following main conclusions can be drawn:

a) Sideslip angle does not practically affect the lift coefficient except at high angles of attack and high banking angles. The strake vortex tends to delay wing vortex breakdown caused by small variations in sideslip and/or banking angles.
b) Lateral manoeuvres at low speeds must be executed at high angles of attack in order to compensate the loss in the lift coefficient.
c) As the sideslip or banking angle increases, the minimum drag angle of attack increases while the value of the minimum drag and the maximum lift to drag ratio decrease. The drag at zero lift and the value of the lift at the minimum drag point are less affected by lateral manoeuvres, specially at high Reynolds numbers.
d) The bank angle slightly degrades the stability margin and displaces the equilibrium point towards negative lift coefficients. The sideslip angle effect is only noticed at low Reynolds numbers where it tends to degrade the stability margin but slightly affects the equilibrium point.
e) The sideslip angle adds a practically constant negative side force over the range of the angles of attack under consideration. This value increases as the bank angle increases.
f) A negative stabilizing rolling moment is added by the bank angle and the sideslip angle at moderate and high angles of attack, while at low angles of attack the contributions of these angles are small.
g) The Bank angle adds a positive yawing moment at low angles of attack and a negative yawing moment at high angles of attack. The angle of attack for which the change in the bank angle has no yawing moment contribution, depends, mainly, on the sideslip angle and, to a very small extent on the Reynolds number.

## REFERENCES

1. Reddy, C.S., "Effect of Leading Edge Vortex Flap On Aerodynamic Performance of Delta Wings," J. of Aircraft, Vol. 18, pp. 796-798, (1981).
2. Earnshaw, P. B. and Lawford, J. A., "Low-Speed-Wind-Tunnel Experiments on a Series of Sharp-Edged Delta Wings," Aeronautical Research Council, R&M No. 3424, (1966).
3. Wentz, W. H. and McMahon, M. C., "An Experimental Investigation of the Flow Fields about Delta and Double Delta Wings at Low Speeds," NASA CR 521, Aug. (1966).

4. Rolls, L. S., Koenig, D. G. and Drinkwater, J. F. III, "Flight Investigation of the Aerodynamic Properties of an Ogee Wing," NASA TN D-3071, Dec. (1965).
5. Skow, A. M. and Erikson, G. E., "Modern Fighter Aircraft Design for High Angle-of- Attack Maneuvering," AGARD LS-121, March (1982).
6. Lamar, J. E. and Frink, N. T., "Experimental and Analytical Study of the Longitudinal Aerodynamic Characteristics of Analytically and mpirically Designed Strake Wing Configurations at Subcritical Speeds," NASA TP-1803, June (1981).
7. Lamar, J. E. and Frink, N. T., "Aerodynamic Features of Designed Strake-Wing Configurations," J. of Aircraft, Vol 19, pp. 639-646, (1982).
8. Luckring, J. M., "Aerodynamics of Strake-Wing Interactions," J. of Aircraft, Vol. 16, pp. 756-762, (1979).
9. Wedmeyer, E. H., "Stable and Unstable Vortex Separation," AGARD CP-274, Jan. (1979).
10. Fiddes, S. P. and Smith, J. H. B., " Strake Induced Separation at Moderately Swept Leading Edges," RAE TR-77128, (1977).
11. Stallings, R. L. Jr., "Low Aspect Ratio Wings at High Angles of Attack", Tactical Missile Aerodynamics, Edited by M. J. Hemsch and J. N. Nielsen, Vol. 12. Progress in Astronautics and Aeronautics, Published by AIAA, Inc. Washington, chapter III, pp. 89-128, (1986).
12. Brennenstuhl, U. and Hummel, D., "Vortical Formation over Double-Delta Wings," ICAS-82-6.6.3, Aug. (1982).
13. Verhaagen, N. G., "An Experimental Investigation of Vortex Flow Over Delta and Double-Delta Wings at Low speed," AGARD CP-342, Paper 7, April (1983).
14. Hoeijmakers, H. W. M., Vaatstra, W. and Verhaagen, N. G., "Vortex Flow Over Delta and Double-Delta Wings," J. of Aircraft, Vol. 20, pp. 825-832, (1983).
15. Hsu, C.-H., Hartwich, P.-M. and Liu, C. H., "Computation of Vortical Interaction for Sharp-Edged Double-Delta Wing," J. of Aircraft, Vol. 25, pp. 442-447,(1988).
16. Smith, C. W. and Anderson, C. A., "Design Guidelines for Application Forebody and Nose Strakes to a Fighter Aircraft Based on F-16 Wind Tunnel Testing Experience," AGARD CP-147, Jan. (1979).
17. Frink, N. T. and Lamar, J. E., "Water Tunnel and Analytical Investigation of the Effect of Strake Design Variables on Strake Vortex Breakdown Characteristics," NASA TP-1676, Aug. (1980).
18. Zohar, Y. and Er-El, J.,"Influence of tha Aspect Ratio on the Aerodynamics of the Delta Wing at High Angle of Attack," Journal of Aircraft, Vol.25, No.3, pp200-205, (1988).